

Helmholtz solitons: Maxwell equations, interface geometries and vector regimes

Pedro Chamorro-Posada¹, Julio Sánchez-Curto¹, James M. Christian², Graham S. McDonald²

¹ Departamento de Teoría de la Señal y Comunicaciones e Ingeniería Telemática,
Universidad de Valladolid, ETSI Telecomunicación,
Campus Miguel Delibes s/n, Valladolid 47011, Spain.

Phone: +34-983-42185545, Fax: +34-983-423667, e-mail: pedcha@tel.uva.es

² Joule Physics Laboratory, School of Computing, Science and Engineering,
Institute for Materials Research,

University of Salford, Salford M5 4WT, UK

Phone : +44-161-295-5079, Fax: +44-161-295-5575, e-mail: g.s.mcdonald@salford.ac.uk

ABSTRACT

In this paper, we give an overview of new results in Helmholtz soliton theory. Firstly, fundamental considerations are made in terms of new contexts for Helmholtz solitons that arise directly from Maxwell's equations. We then detail applications involving a variety of different material interfaces and the role of Helmholtz solitons in these configurations. Finally, specific new families of solutions arising from the generalisation of the Manakov equation are reported.

Keywords: Spatial optical solitons, nonlinear Helmholtz equation, non-paraxiality, time-domain simulation.

1. INTRODUCTION

Previous research on the Non-Linear Helmholtz (NLH) equation has permitted the generalization of both bright [1] and dark [2] spatial solitons in Kerr media to the finite-angle regime, where oblique beam propagation may be at an *arbitrarily large angle* relative to the longitudinal axis. In this approach, the intrinsic angular limitations of conventional Non-Linear Schrödinger (NLS) analyses, imposed by the assumption of beam paraxiality, are eliminated. Our analytical investigations are complimented by well-tested numerical techniques, developed specifically for the accurate solution of NLH equations [3].

The Kerr NLH equation is fully equivalent [1] to a non-paraxial Non-Linear Schrödinger equation

$$\kappa \frac{\partial^2 u}{\partial \zeta^2} + i \frac{\partial u}{\partial \zeta} + \frac{1}{2} \frac{\partial^2 u}{\partial \xi^2} \pm |u|^2 u = 0, \quad (1)$$

describing the evolution of the normalized complex envelope u of an optical beam. Here, $\zeta = z/L_D$, $\xi = 2^{1/2} x/w_0$, $L_D = kw_0^2/2$, $\tilde{E}(x, z) = E_0 u(x, z) \exp(ikz)$ and $k = 2\pi/\lambda$. n_0 is the linear refractive index, $\lambda = \lambda_0/n_0$ the optical wavelength, $E_0 = (n_0/k|n_2|L_D)^{1/2}$, n_2 the Kerr coefficient and $\kappa = 1/k^2 w_0^2$ is the non-paraxiality parameter. The \pm sign flags a focusing or defocusing Kerr non-linearity. Equation (1) retains the full spatial symmetry of the NLH model, and is a more convenient framework for comparing new results with those obtained from paraxial calculations. The NLS equation can be recovered from Eq. (1) when the Helmholtz operator $\kappa \partial_{\zeta\zeta}^2$ is neglected.

In this paper, we give an overview of some recent new results in Helmholtz soliton theory. Three topics have been selected for this purpose. We consider the modeling of the propagation properties of Helmholtz solitons directly using the full 2D Maxwell's equations [4], the behaviour of solitons incident on non-linear interfaces at oblique angles [5], and families of new exact analytical vector solitons arising from the proposed Helmholtz-Manakov (H-M) equation [6].

The use of the full 2D non-linear Maxwell's equations for analyzing the propagation properties of Helmholtz solitons provides a more general framework free of the restrictions encountered in other approaches. The results support investigations based on Eq. (1) for TE-polarized optical beams in a quasi-2D medium, and allow us to extend previous work on Helmholtz solitons to non-paraxial regimes other than those arising solely from angular considerations.

The reflection and refraction properties of soliton beams at non-linear interfaces have been analyzed extensively using the paraxial NLS equation [7]. Here, we present new results concerning the non-linear reflection and refraction properties of optical solitons, at *arbitrary* angles of incidence, using an NLH model. Our work highlights the limitations of previous studies based on the NLS equation that are restricted, by the paraxial approximation, to consideration of vanishingly-small incidence angles.

The propagation of spatial vector soliton beams is often described by the Manakov equation [8]. We report the Helmholtz generalization of the Manakov model and present its exact analytical soliton solutions, derived for both focusing and defocusing Kerr media. These results are accompanied by an overview of the dynamical properties of the new solutions. Helmholtz-Manakov solitons are found to exhibit non-trivial features that are absent from the corresponding paraxial-based descriptions.

2. HELMHOLTZ SOLITONS AND MAXWELL EQUATIONS

The evolution of a TE-polarized optical field, propagating in a non-magnetic two-dimensional medium with electric field $\mathbf{E}(x, z, t) = \hat{\mathbf{y}}E_y(x, z, t)$, is described by the 2D Maxwell equations

$$\frac{\partial E_y}{\partial x} = -\mu_0 \frac{\partial H_z}{\partial t}, \quad \frac{\partial E_y}{\partial z} = \mu_0 \frac{\partial H_x}{\partial t} \quad \text{and} \quad \frac{\partial H_x}{\partial z} - \frac{\partial H_z}{\partial x} = \epsilon_0 n^2 \frac{\partial E_y}{\partial t}, \quad (2)$$

for beam propagation that takes place in the x - z plane. In a Kerr medium, the refractive index is

$$n^2 = n_0^2 + \delta_{\text{NL}}(E_y), \quad (3)$$

where the nonlinear contribution to the refractive index is $\delta_{\text{NL}} \approx 2n_0^2 n_2 E_y^2$ for an instantaneous response medium. In slow response nonlinear media, where the nonlinearity cannot respond at optical frequencies, we have $\delta_{\text{NL}} \approx 2n_0^2 n_2 \langle E_y^2 \rangle$, where the braces indicate temporal average over a large number of optical cycles [9]. Such behaviour can be implemented by supplementing Eqs. (2) and (3) with a Debye type of equation for the nonlinear contribution to the refractive index [10]. In either case, we report that, for a continuous-wave beam, a NLH equation can be derived from Eqs. (2) and (3). This equation governs the evolution of the complex amplitude $\tilde{E}(x, z)$ of the optical field, where $E_y(x, z, t) = \text{Re}[\tilde{E}(x, z)\exp(-i\omega_0 t)]$. Equation (1) is obtained as the corresponding evolution equation for the field envelope.

The behaviour of multi-soliton solutions of the NLS equation can be strongly influenced by the presence of perturbations. Helmholtz-type non-paraxiality acts as such a perturbative contribution during the initial focusing stages of periodic evolution [11]. Equation (1) predicts that the Helmholtz operator $\kappa \partial_{\zeta\zeta}$ modifies the soliton period [11] of a two-soliton bound state, and this has been confirmed by numerical solution of the full Maxwell equations [4,12].

When even stronger non-paraxiality is present, a launched high-order soliton can become unstable and undergo a fission effect, whereby the bound state breaks up into its individual components [11]. Figure 1 illustrates the splitting of a third-order soliton beam into three fundamental Helmholtz solitons, as given by Eq. (1) when $\kappa = 0.005$ [9]. Figure 2.a displays the electric field amplitude at a given time t_0 , obtained by solving the full Maxwell's equations assuming an instantaneous nonlinearity. Whereas the two results agree qualitatively in the description of a fission process, there are noticeable differences in the detailed evolution for the two cases. These differences have their origin in the presence of parametric conversion to the third harmonic in the strong focusing stages when the full time domain Maxwell equations are used to describe the problem. This effect, which is not taken into account in Eq. (1), where a single spectral component is considered,

acts as a loss mechanism on the fundamental frequency component beam and, thus, introduces an additional perturbation which modifies the propagation properties of the optical beam.

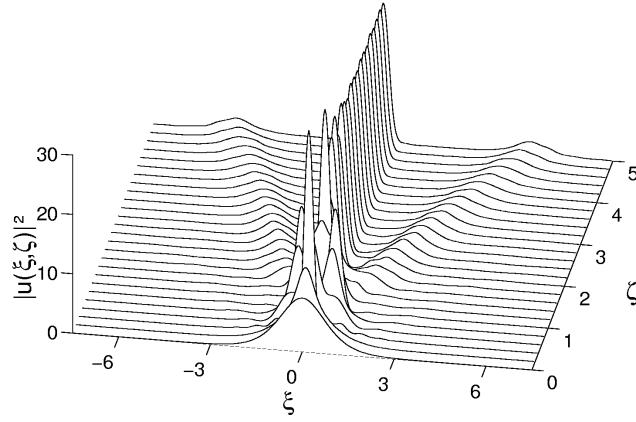


Figure 1. Evolution of an optical beam showing the splitting of a third-order soliton [11] as obtained from the numerical integration of Eq. (1).

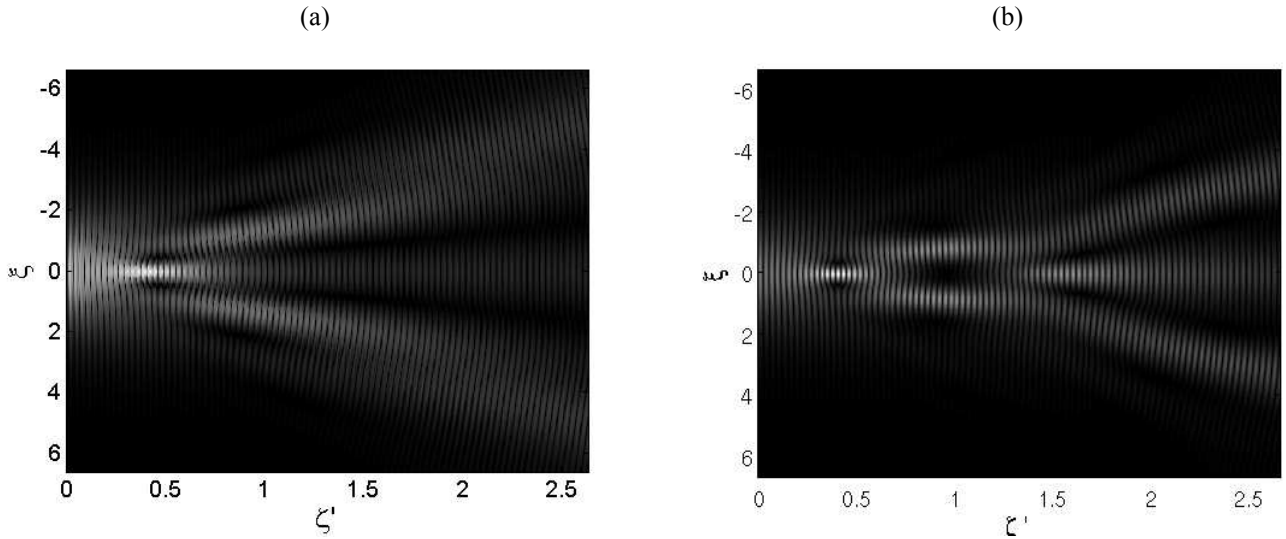


Figure 2. E field magnitude $|E_y(\xi, \zeta, t_0)|$ computed from the time-domain Maxwell's equations for a nonlinear instantaneous response medium (a) and a slow response nonlinear medium (b). In the calculations, equal scalings have been used for the $\xi = 2^{1/2}x/w_0$ and $\zeta = 2^{1/2}z/w_0$ coordinates. The ζ coordinate has been adjusted to that of Figure 2 by using $\zeta' = (2\kappa)^{1/2} \zeta$.

The third harmonic generation due to four-wave mixing (FWM) can be prevented by assuming a slow nonlinear response. Figure 2.b shows the computed electric field at t_0 amplitude for a medium with an arbitrary second order response of the nonlinear contribution of the refractive index which has been designed to prevent the generation of FWM terms and, at the same time, provide a controllable response time. We find that the description of the fission process at a given instant and in the region of space shown in Figure 2 is in excellent agreement with the results obtained using the CW Eq. 1. Never-

theless, the detailed temporal evolution is found to exhibit rich dynamics, dominated by the selected response time for the nonlinear refractive index, which shows a deep contrast with the straightforward evolution found for an instantaneous response medium.

3. HELMHOLTZ SOLITONS AT NON-LINEAR INTERFACES

The oblique evolution of solitons at the interface separating two Kerr-type media can be described by a generalized NLH equation [5]. Our numerical simulations show that, when there is a mismatch only in the linear part of the refractive index, the incident solitons are governed by Snell's law [5]. In general, it has been found that the reflection and refraction characteristics of optical solitons possess key features that cannot be adequately described by paraxial theory [7].

In this paper, we focus primarily on the analysis of soliton behaviour when the linear refractive index is continuous across the interface. The general solution shows that, when a soliton enters a medium with a weaker non-linearity, the outgoing beam may suffer diffractive spreading without limit unless the input power exceeds some critical value (see Fig. 2(a)). On the other hand, when the second medium is characterized by a stronger non-linearity, any excess power associated with the incident soliton causes the beam to break up into a distribution of narrower solitons (see Fig. 2(b)).

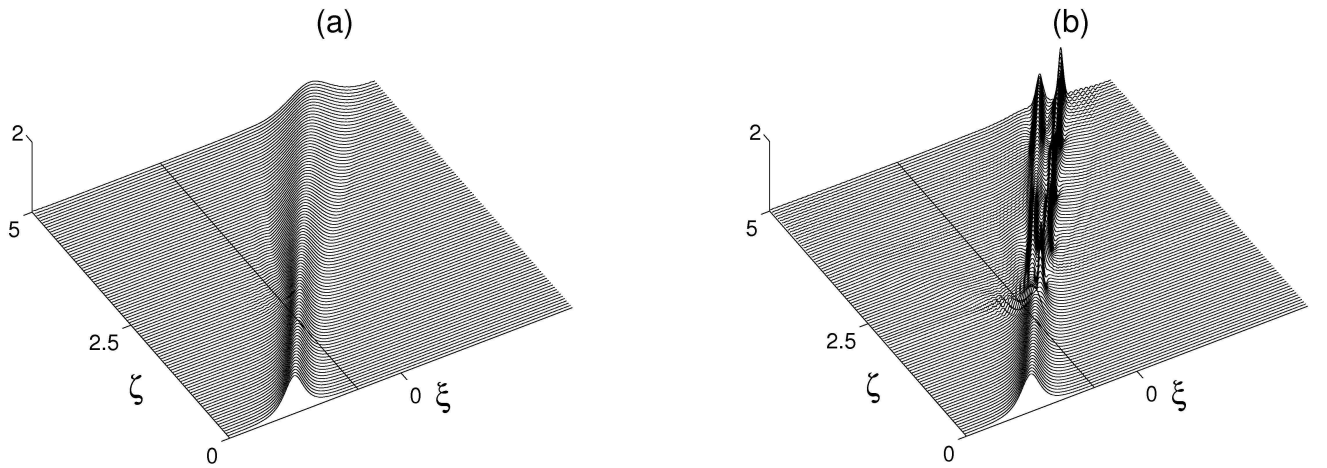


Figure 3. Numerical results corresponding to soliton evolution at the interface between two Kerr-type media when the magnitude of the non-linear refractive index in the second medium is (a) lower and (b) higher than in the first medium.

The Helmholtz-interface framework yields important quantitative corrections to paraxial predictions [7] that can exceed 100%. Moreover, significant qualitative differences between the two descriptions appear when the magnitude of the non-linearity is higher in the second medium. In the paraxial regime, the number of secondary solitons increases depending on the magnitude of the square root of an expression involving the two non-linear indexes. Helmholtz modelling shows that a more restrictive number of solitons are actually formed. We also find that the multi-soliton structure that develops depends not only on the aforementioned index relationship but also on the angle of incidence. In a pending publication [5], we present a full characterization of the soliton pattern generated in the second medium based on extensive numerical simulation.

4. HELMHOLTZ-MANAKOV SOLITONS

When the electric field confined to an isotropic quasi-2D waveguide has only a single transverse field component, the NLH equation (1) provides an accurate description of scalar wave propagation. When the guided field has two orthogonal transverse components, the appropriate model is the Helmholtz-Manakov (H-M) equation [6],

$$\kappa \frac{\partial^2 \mathbf{U}}{\partial \zeta^2} + i \frac{\partial \mathbf{U}}{\partial \zeta} + \frac{1}{2} \frac{\partial^2 \mathbf{U}}{\partial \xi^2} \pm (\mathbf{U}^\dagger \mathbf{U}) \mathbf{U} = \mathbf{0}. \quad (4)$$

The physical scalings are identical to those used in Eq. (1), but now the wave field \mathbf{U} is the single-column two-component vector $\mathbf{U}(\xi, \zeta) = [A(\xi, \zeta), B(\xi, \zeta)]^T$, where T denotes the transpose. As in the scalar case, the familiar (paraxial) Manakov equation [8] can be recovered in the limit that the consequences of the Helmholtz operator $\kappa \partial_{\zeta\zeta}$ are negligible with respect to other terms. The H-M equation possesses $U(2)$ symmetry, and the evolution of the two perpendicular field components involves a non-linear coupling due to the Kerr effect.

Equation (4) admits four new exact analytical soliton solutions, which have been deriving by combining ansatz techniques and Hirota's method [13] with the physical geometry of the propagation problem [2,11]. In both focusing and defocusing cases, there are two distinct solution families. In a focusing Kerr medium, we find bright-bright and bright-dark solitons, where the primary component A is always a bright (*sech*-type) Helmholtz soliton, and the secondary B is a bright and a black (*tanh*-type) structure, respectively. In the defocusing case, we have dark-bright and dark-dark solitons. The new vector solutions capture all the generic physical attributes of Helmholtz scalar solitons [1,2]. These include angular beam broadening, modifications to the beam phase and non-trivial corrections to intrinsic velocities. An important point to note is that the bright-dark and dark-bright solutions are not equivalent; they have very different stability properties.

4.1 New families of Helmholtz solitons

We first consider the solutions for a focusing medium. These can be derived using an ansatz approach to find the on-axis beam, and then applying an orthogonal transformation to generate the desired off-axis solution. Taking the +ve sign in Eq. (4), we find that the bright-bright family comprises a Helmholtz bright soliton in each component,

$$\mathbf{U}(\xi, \zeta) = \mathbf{C} \eta \operatorname{sech} \left[\frac{\eta(\xi + V\zeta)}{\sqrt{1 + 2\kappa V^2}} \right] \exp \left[i \sqrt{\frac{1 + 2\kappa\eta^2}{1 + 2\kappa V^2}} \left(-V\xi + \frac{\zeta}{2\kappa} \right) \right] \exp \left(-i \frac{\zeta}{2\kappa} \right), \quad (5)$$

The matrix $\mathbf{C} = [\exp(i\delta_1) \cos \alpha, \exp(i\delta_2) \sin \alpha]^T$ is a complex polarization vector obeying $\mathbf{C}^\dagger \mathbf{C} = 1$. The free parameter α is the polarization angle, determining the relative strength of the excitation in each component, and δ_j ($j = 1, 2$) are phases. In the limit that $\alpha \rightarrow 0$, or $\pi/2$, the NLH bright soliton [1] is recovered. The bright-dark soliton solution is,

$$A(\xi, \zeta) = \eta \operatorname{sech} \left[\frac{a(\xi + V\zeta)}{\sqrt{1 + 2\kappa V^2}} \right] \exp \left[i \sqrt{\frac{1 + 2\kappa\eta^2}{1 + 2\kappa V^2}} \left(-V\xi + \frac{\zeta}{2\kappa} \right) \right] \exp \left(-i \frac{\zeta}{2\kappa} \right), \quad (6a)$$

$$B(\xi, \zeta) = \sqrt{\eta^2 - a^2} \tanh \left[\frac{a(\xi + V\zeta)}{\sqrt{1 + 2\kappa V^2}} \right] \exp \left[i \sqrt{\frac{1 + 4\kappa(\eta^2 - a^2)}{1 + 2\kappa V^2}} \left(-V\xi + \frac{\zeta}{2\kappa} \right) \right] \exp \left(-i \frac{\zeta}{2\kappa} \right). \quad (6b)$$

where $\eta^2 > a^2$. Solution (6) consists of a bright soliton in the primary component, and a dark-type *tanh* solution (with a phase shift of π across its transverse dimension) in the secondary component. The bright soliton of Eq. (1) can be recovered in the limit $a \rightarrow \eta$. The transverse velocity V of the beam is directly related to the propagation angle θ . This particular relation takes the same form as that linking the analogous properties of the dark-bright soliton discussed below.

For a defocusing medium, where the -ve sign is taken in Eq. (4), we have derived dark-bright and dark-dark soliton solution families. The dark-bright soliton is,

$$A(\xi, \zeta) = A_0 \left[\cos \phi \tanh \left[\frac{a(\xi + W\zeta)}{\sqrt{1 + 2\kappa W^2}} \right] + i \sin \phi \right] \exp \left[i \sqrt{\frac{1 - 4\kappa A_0^2}{1 + 2\kappa W^2}} \left(-V\xi + \frac{\zeta}{2\kappa} \right) \right] \exp \left(-i \frac{\zeta}{2\kappa} \right), \quad (7a)$$

$$B(\xi, \zeta) = \sqrt{A_0^2 \cos^2 \phi - a^2} \operatorname{sech} \left[\frac{a(\xi + W\zeta)}{\sqrt{1 + 2\kappa W^2}} \right] \exp \left[i \sqrt{\frac{1 - 4\kappa \left(A_0^2 - \frac{1}{2} a^2 \right)}{1 + 2\kappa W^2}} \left(-W\xi + \frac{\zeta}{2\kappa} \right) \right] \exp \left(-i \frac{\zeta}{2\kappa} \right). \quad (7b)$$

The transverse velocity V is related to the propagation direction θ , relative to the longitudinal z axis, of the background plane wave through $\tan \theta = \sqrt{2\kappa}V$. The intrinsic velocity V_0 is related to the propagation direction θ_0 , relative to the plane-wave background, of the grey ‘‘dip’’ through $\tan \theta_0 = \sqrt{2\kappa}V_0$. W is the net velocity of the beam, where $\tan(\theta - \theta_0) = \sqrt{2\kappa}W$. It can then be shown that,

$$W = \frac{V - V_0}{1 + 2\kappa V V_0}, \quad (7c)$$

and

$$V_0(\phi) = \frac{a \tan \phi}{\sqrt{1 - 2\kappa(2\chi^2 + a^2 \tan^2 \phi)}}, \quad (7d)$$

where $\chi^2 \equiv A_0^2$. Inspection of Eq. (7d) shows that there is a maximum phase shift (that is, ‘‘greyness’’) that the solution can support, depending upon the non-paraxial parameter κ , the background intensity A_0^2 and the free parameter a . That is,

$$\tan \phi_{\max} = \sqrt{\frac{1 - 4\kappa\chi^2}{2\kappa a^2}}. \quad (8)$$

The physical origin of this effect is the requirement that the refractive index must remain positive, or, equivalently, that the non-linear phase shift must not exceed the linear one [2]. There is no analogue of this effect in paraxial theory, since conventional Manakov solitons may possess any arbitrary $0 \leq |\phi| \leq \pi/2$ [14]. Solution (7) is also constrained by $A_0^2 \cos^2 \phi \geq a^2$. When the equality is satisfied, the bright component vanishes and dark soliton of Eq. (1) is recovered [2].

The dark-dark soliton of Eq. (4) is,

$$A(\xi, \zeta) = A_0 \left[\cos \phi_1 \tanh \left[\frac{a(\xi + W\zeta)}{\sqrt{1 + 2\kappa W^2}} \right] + i \sin \phi_1 \right] \exp \left[i \sqrt{\frac{1 - 4\kappa\chi^2}{1 + 2\kappa V_1^2}} \left(-V_1\xi + \frac{\zeta}{2\kappa} \right) \right] \exp \left(-i \frac{\zeta}{2\kappa} \right), \quad (9a)$$

$$B(\xi, \zeta) = B_0 \left[\cos \phi_2 \tanh \left[\frac{a(\xi + W\zeta)}{\sqrt{1 + 2\kappa W^2}} \right] + i \sin \phi_2 \right] \exp \left[i \sqrt{\frac{1 - 4\kappa\chi^2}{1 + 2\kappa V_2^2}} \left(-V_2\xi + \frac{\zeta}{2\kappa} \right) \right] \exp \left(-i \frac{\zeta}{2\kappa} \right), \quad (9b)$$

where $\chi^2 \equiv A_0^2 + B_0^2$. The structure of this solution is the most complicated, with two possible transverse velocity parameters V_j ($j=1,2$) and two intrinsic velocities given by Eq. (7d), where $V_{0j}(\phi_j) = V_0(\phi \rightarrow \phi_j)$. However, there must be a common *net* velocity W . Again, each component of the solution can sustain a maximum greyness, given by Eq. (8).

In each of the four new solutions presented above, the corresponding Manakov solitons [8,14] can be recovered in the *simultaneous* multiple limits $\kappa \rightarrow 0$ (broad beams), $\kappa I \rightarrow 0$ where $I \equiv \{\eta^2, A_0^2, B_0^2\}$ (low intensity), and $\kappa v^2 \rightarrow 0$

where $\nu = \{V, V_0, W\}$ (negligible propagation angles). This is a physical requirement of Helmholtz soliton theory, since paraxial solutions must be found when the system behaves paraxially. The simultaneous limits are completely equivalent to $|\kappa \partial_{\zeta \zeta}| \rightarrow 0$.

4.2 Helmholtz-Manakov soliton stability

We now present an overview of the stability properties of the new families H-M solitons, with respect to perturbations to their angular spectra. In focusing media, we examine the stability of bright-bright solitons by considering initial conditions of the form $U(\xi, 0) = C \operatorname{sech}(\xi) \exp(-iS_0 \xi)$, that corresponds to launching an exact solution of the (paraxial) Manakov equation when $\eta = 1$ [8]. For such beams, with $\kappa \ll 1$ and $\kappa \eta^2 \ll 1$, rotational transformation (that gives a new longitudinal axis coinciding with the propagation axis) shows that each initial condition may be regarded as an exact Manakov soliton whose width has been reduced by the Helmholtz factor $(1 + 2\kappa V^2)^{1/2}$, where $V = S_0 (1 - 2\kappa S_0^2)^{-1/2}$ [11]. For $S_0 = 5, 10$ and 15 , with a typical value of $\kappa = 10^{-3}$, the non-paraxial propagation angles are $\theta = 12.9^\circ, 26.6^\circ$ and 42.1° . The peak amplitude exhibits monotonically-decreasing oscillations of the same nature as those reported for scalar Helmholtz solitons [2,11]. As $\zeta \rightarrow \infty$, the oscillations disappear, leaving a stationary beam. This final, propagation-invariant, state is an exact H-M soliton. We have also considered similar initial conditions for the bright-dark soliton (6) and have found that such perturbed beams are always unstable.

For defocusing media, we consider the canonical dark-bright initial condition,

$$A(\xi, 0) = \tanh(a\xi) \exp(-iS_0 \xi), \quad (10a)$$

$$B(\xi, 0) = \sqrt{1 - a^2} \operatorname{sech}(a\xi) \exp(-iS_0 \xi). \quad (10b)$$

Figure 4 illustrates the evolution of the beam amplitude and width for two values of a . An H-M soliton is always found to emerge asymptotically from initial condition (10).

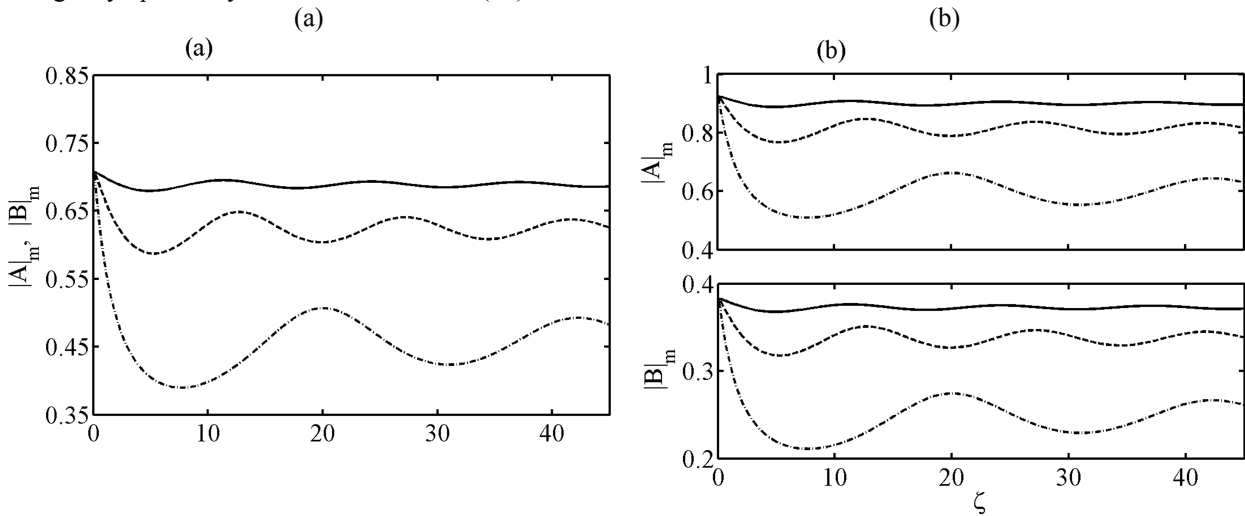


Figure 4. Reshaping curves for initial condition (10) with (a) $a = 0.8$ and (b) $a = 0.2$.
Solid curves: $S_0 = 5$, dashed curves: $S_0 = 10$, dot-dash curves: $S_0 = 15$.

We have also considered dark-dark initial conditions for defocusing media,

$$A(\xi, 0) = A_0 \tanh(\xi) \exp(-iS_0 \xi), \quad (11a)$$

$$B(\xi, 0) = \sqrt{1 - A_0^2} \tanh(\xi) \exp(-iS_0 \xi), \quad (11b)$$

Figure 5 illustrates the reshaping process, and demonstrates the relatively rapid emergence of full H-M solitons from such initial conditions. The asymptotic width of the beam in these cases is given by $(1 + 2\kappa V^2)^{1/2}$, and is independent of the amplitude A_0 , so long as the quasi-paraxial condition $\kappa A_0^2 \ll 1$ is satisfied.

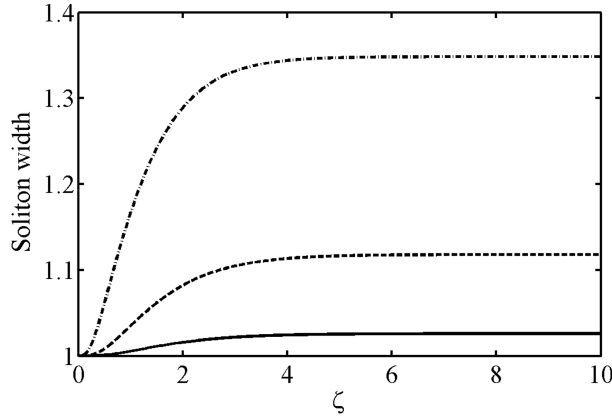


Figure 5. Universal reshaping curves for initial condition (11). Solid curves: $S_0 = 5$, dashed curves: $S_0 = 10$, dot-dash curves: $S_0 = 15$.

CONCLUSIONS

Firstly, we have shown that exact analytical Helmholtz soliton solutions satisfy a governing evolution equation that follows *exactly* from 2D Maxwell's equations. This result generalizes significantly the domain of applicability of Helmholtz soliton theory to beyond non-paraxial considerations arising from oblique propagation effects. These analytical conclusions are substantiated by comparisons of the numerical solutions of the appropriate non-linear Helmholtz equation and those of Maxwell's equations.

We then presented results from the first analysis of solitons incident at non-trivial oblique angles on interfaces separating two different Kerr media. This regime is of fundamental interest and, as is shown in Fig. 2, is clearly outside the scope of approaches based on the paraxial approximation [7]. These preliminary interface results can be generalized in a systematic way by considering solitons in other classes of media, such as power-law and polynomial-type media [15].

Finally, we reported a new soliton-bearing vector wave equation for describing the propagation of spatial optical beams in isotropic Kerr media. Hirota's method and geometrical considerations have allowed us to derive families of four new exact analytical soliton solutions. The known Manakov solitons, along with scalar paraxial Kerr and scalar Helmholtz Kerr solitons, emerge as particular limits of these more general Helmholtz solutions. A numerical perturbative analysis has allowed us to examine the stability of these new vector solitons. With the exception of the bright-dark class of soliton, they all behave as robust attractors and can be classified as stable fixed points of the system (in a non-linear dynamical sense).

We expect the new Helmholtz-Manakov equation, and its soliton solutions, to form the basis for a thorough understanding of how multiple spatial vector beams interact with each other at arbitrarily large angles [16]. Furthermore, these considerations are likely to play a central role in the analysis of other experimentally relevant configurations, such as the oblique propagation and interaction of spatial solitons at arbitrary angles in birefringent waveguides. Helmholtz-type models provide an ideal framework for investigating the finite-angle dependence of many vectorial phenomena, that include beams incident obliquely on non-linear interfaces, polarization scattering effects, and polarization instabilities (transfer of energy from the fast to the slow mode) in birefringent slab waveguides [17,18]. Our considerations are also likely to be of central importance in the design of any futuristic all-optical devices that exploit multiplexed spatial solitons for their operation.

ACKNOWLEDGEMENTS

This work has been funded by MCyT and FEDER, grant number TIC 2003-07020 and JCyL grant number VA083A05, and the Institute for Materials Research of the University of Salford.

REFERENCES

1. P. Chamorro-Posada, G. S. McDonald, G. H. C. New, "Exact soliton solutions of the nonlinear Helmholtz equation: communication," *J. Opt. Soc. Am. B*, vol. 19, p. 1216, 2002.
2. P. Chamorro-Posada and G. S. McDonald, "Helmholtz dark solitons," *Opt. Lett.*, vol. 15, p. 827, 2003.
3. P. Chamorro-Posada, G. S. McDonald and G. H. C. New, "Non-paraxial beam propagation methods," *Opt. Commun.*, vol. 19, p. 1, 2001.
4. P. Chamorro-Posada and G. S. McDonald, "Analysis of the propagation properties of Helmholtz solitons using Maxwell equations," *submitted*.
5. J. Sánchez-Curto, P. Chamorro-Posada and G. S. McDonald, "Helmholtz solitons at nonlinear interfaces," *submitted*.
6. J. M. Christian, G. S. McDonald and P. Chamorro-Posada, "Helmholtz-Manakov solitons," *submitted*.
7. A. B. Aceves, J. V. Moloney and A. C. Newell, "Theory of light-beam propagation at nonlinear interfaces. I. Equivalent-particle theory for a single interface," *Phys. Rev. A*, vol. 39, p. 1809, 1989.
8. S. V. Manakov, "On the theory of two-dimensional stationary self-focusing of electromagnetic waves," *Sov. Phys. JETP*, vol. 38, p. 248, 1974.
9. A. Yariv, *Quantum Electronics*, Third Ed., John Wiley & Sons, 1989.
10. A.C. Newell and J.V. Moloney, *Nonlinear Optics*, Addison-Wesley, 1992.
11. P. Chamorro-Posada, G. S. McDonald and G. H. C. New, "Propagation properties of non-paraxial spatial solitons," *J. Mod. Opt.*, vol. 47, p. 1877, 2000.
12. R. M. Joseph and A. Taflove, "Spatial soliton deflection mechanism indicated by FD-TD Maxwell's equations modeling," *IEEE Photon. Technol. Lett.*, vol. 6, p. 1251, 1994.
13. R. Hirota, "Exact envelope-soliton solutions of a nonlinear wave equation," *J. Math. Phys.*, vol. 14, p. 805, 1973.
14. A. P. Sheppard and Y. S. Kivshar, "Polarized dark solitons in isotropic Kerr media," *Phys. Rev. E*, vol. 55, p. 4773, 1997.
15. J. M. Christian, G. S. McDonald and P. Chamorro-Posada, manuscripts in preparation.
16. P. Chamorro-Posada and G. S. McDonald, "Spatial Kerr soliton collisions at arbitrary angles," *submitted*.
17. R. R. Malendevich, L. Friedrich, G. I. Stegeman, J. M Soto-Crespo, N. N. Akhmediev and J. S. Aitchison, "Radiation-related polarization instability of Kerr spatial vector solitons," *J. Opt. Soc. Am. B* vol. 19, p. 695, 2002.
18. L. Friedrich, R. Malendevich, G. I. Stegeman, J. M. Soto-Crespo, N. N. Akhmediev and J. S. Aitchison, "Radiation related polarization instability of fast Kerr spatial solitons in slab waveguides," *Opt. Commun.* vol. 186, 335, 2000.